Electron beam induced coloration and luminescence in layered structure of WO 3 thin films grown by pulsed dc magnetron sputtering

A. Karuppasamy and A. Subrahmanyam

Citation: Journal of Applied Physics **101**, 113522 (2007); doi: 10.1063/1.2737957
View online: http://dx.doi.org/10.1063/1.2737957
View Table of Contents: http://scitation.aip.org/content/aip/journal/jap/101/11?ver=pdfcov
Published by the AIP Publishing

Electron beam induced coloration and luminescence in layered structure of WO_3 thin films grown by pulsed dc magnetron sputtering

A. Karuppasamy[a] and A. Subrahmanyam
Semiconductor Laboratory, Department of Physics, Indian Institute of Technology Madras, Chennai-600036, India

(Received 28 January 2007; accepted 4 April 2007; published online 8 June 2007)

Tungsten oxide thin films have been deposited by pulsed dc magnetron sputtering of tungsten in argon and oxygen atmosphere. The as-deposited WO_3 film is amorphous, highly transparent, and shows a layered structure along the edges. In addition, the optical properties of the as-deposited film show a steplike behavior of extinction coefficient. However, the electron beam irradiation (3.0 keV) of the as-deposited films results in crystallization, coloration (deep blue), and luminescence (intense red emission). The above changes in physical properties are attributed to the extraction of oxygen atoms from the sample and the structural modifications induced by electron bombardment. The present method of coloration and luminescence has a potential for fabricating high-density optical data storage device. © *2007 American Institute of Physics*. [DOI: 10.1063/1.2737957]

I. INTRODUCTION

Tungsten oxide is a well-known chromic material that can switch between two optical states in response to an applied dc voltage, UV irradiation, and thermal energy. The coloration behavior of WO_3 is extensively studied due to its potential application in various fields like smart windows, sensors, displays, and automotive rear-view mirrors.[1] The chromic behavior of tungsten oxide has a vast potential in the emerging field of ultrahigh density optical data storage. Once colored, the tungsten oxide has an in-built memory to retain the coloration information even after the source is removed. This property of tungsten oxide, as indicated in the literature,[2,3] makes it a candidate suitable for possible ultrahigh density data storage application. Apart from the above-mentioned conventional methods, WO_3 can also be colored by irradiation methods using electrons, ions, and lasers.[4–6] Recently, the optimization of nanoscale electron emitters (nanotube, nanowire, and nanowires) gives feasibility for high-density data storage based on the electron bombardment of tungsten oxide thin films. In the present Letter, we report the effect of electron bombardment on the structural, morphological, coloration, and luminescent properties of pulsed dc magnetron sputtered WO_3 thin films. We have also proposed the concept for data storage application based on the electron beam induced coloration/luminescence in tungsten oxide thin films.

II. EXPERIMENTAL DETAILS

The layer structured tungsten oxide thin films were deposited on glass substrates by pulsed dc magnetron sputtering of metallic tungsten target in argon and oxygen atmosphere (Advanced Energy, model MDX 500 and MDX Sparc-LE 20 in active arc suppression mode). The sputtering parameters used for the growth of layered structures are sputtering power of $2.0\ W/cm^2$, working pressure (argon +oxygen) of 1.4×10^{-2} mbar (the chamber pressure with argon gas alone is 1.0×10^{-2} mbar), and deposition time of 10 min. The sputtered WO_3 thin films have been irradiated with electron beam in a commercial electron beam evaporation system (Hind Hivac 12A4) at a vacuum of 5.0×10^{-5} mbar. The details about the experimental setup used for electron bombardment is given in our earlier work.[7] In the present study, three samples of size 1.0×1.0 cm have been grown in one run of sputtering. Of the three samples, one is characterized as such and is labeled as S1. The other two samples have been subjected to electron irradiation: sample S2 (bombarded with electron beam of energy 3.5 keV and current of 3.0 mA for 8 s) and sample S3 (bombarded with electron beam of energy 3.5 keV and current of 6.0 mA for 4 s). The crystallinity of the films was studied using Philips X'pert diffractometer. The optical transmittance was recorded using Jasco-V 570 spectrophotometer and the other optical parameters (n,k,t) were determined from the reflectance spectra by Filmetrics-F 20. The chemical composition of the films was investigated by x-ray photoelectron spectroscopy (PHI ESCA system). The surface morphology was studied by scanning electron microscopy (LEO Stereoscan 440) and atomic force microscopy (Digital Instruments Nanoscope IV SPM) measurements. The photoluminescence observations were performed with Jobin-Yvon Fluormax-3.

III. RESULTS AND DISCUSSION

Figure 1 shows the x-ray diffraction pattern of the as-deposited (S1) and electron bombarded tungsten oxide thin films (S2, S3). The broad featureless pattern at lower angles clearly indicates the amorphous nature of as-deposited tungsten oxide thin films. However, the XRD pattern of electron bombarded samples (S2, S3) shows high-intensity peaks corresponding to the tetragonal WO_3 system (JCPDS card No. 89–1287). The samples S2 are found to be highly crystalline with sharp peaks. The highest intensity peak at 24.0° shows preferential orientation along the (100) plane. But, the S3

[a]Author to whom correspondence should be addressed; electronic mail: ksamy@physics.iitm.ac.in

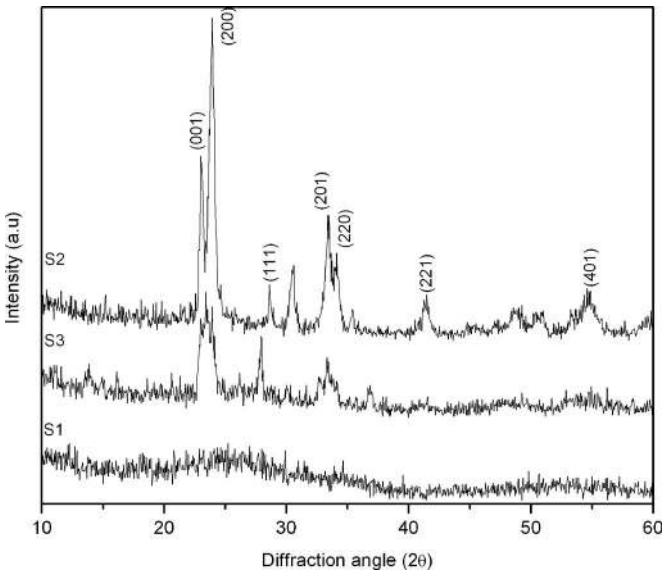

FIG. 1. X-ray diffraction pattern of the as deposited (S1) and electron bombarded (S2, S3) tungsten oxide thin films deposited by pulsed dc magnetron sputtering.

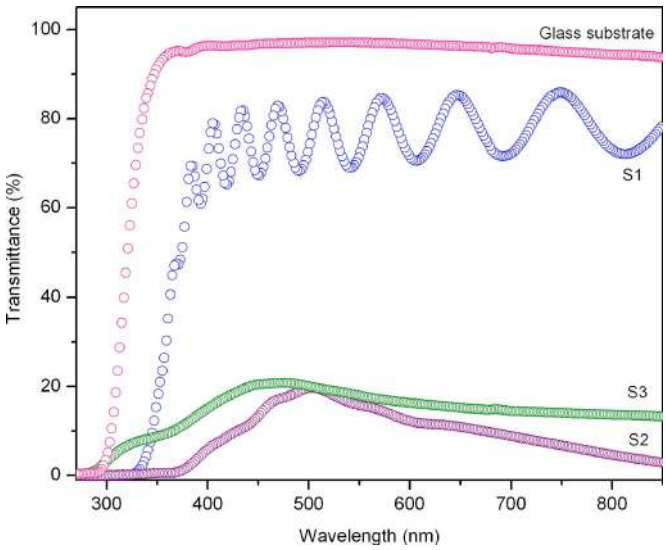

FIG. 2. (Color online) The spectral dependence of transmittance in the wavelength range 250–850 nm for the as-deposited (S1) and electron bombarded (S2, S3) WO_3 thin films.

sample shows broad and less intense peaks, characteristic of nanoscale materials. The average crystallite sizes determined by Scherrer's formula are found to be 40 and 15 nm for S2 and S3 samples, respectively.

The transmittance spectrum of the tungsten oxide thin films (S1–S3) in the wavelength range 250–850 nm is shown in Fig. 2. The spectrum of glass substrate is also presented for reference. The as-deposited WO_3 films have a high transmittance of ~85% in the entire visible range of 400–850 nm. The thickness of the film is 1061 ± 5 nm. The sharp fall in transmittance at $\lambda = 340$ nm corresponds to the fundamental absorption edge of amorphous tungsten oxide. When these samples are bombarded with electron beams, the entire film (1.0×1.0 cm) turns deep blue in S2 sample, showing a maximum transmittance of 15% at $\lambda = 503$ nm. In addition, the band edge is also redshifted by 32 nm. But, in the case of S3 samples, only a portion of the film in and

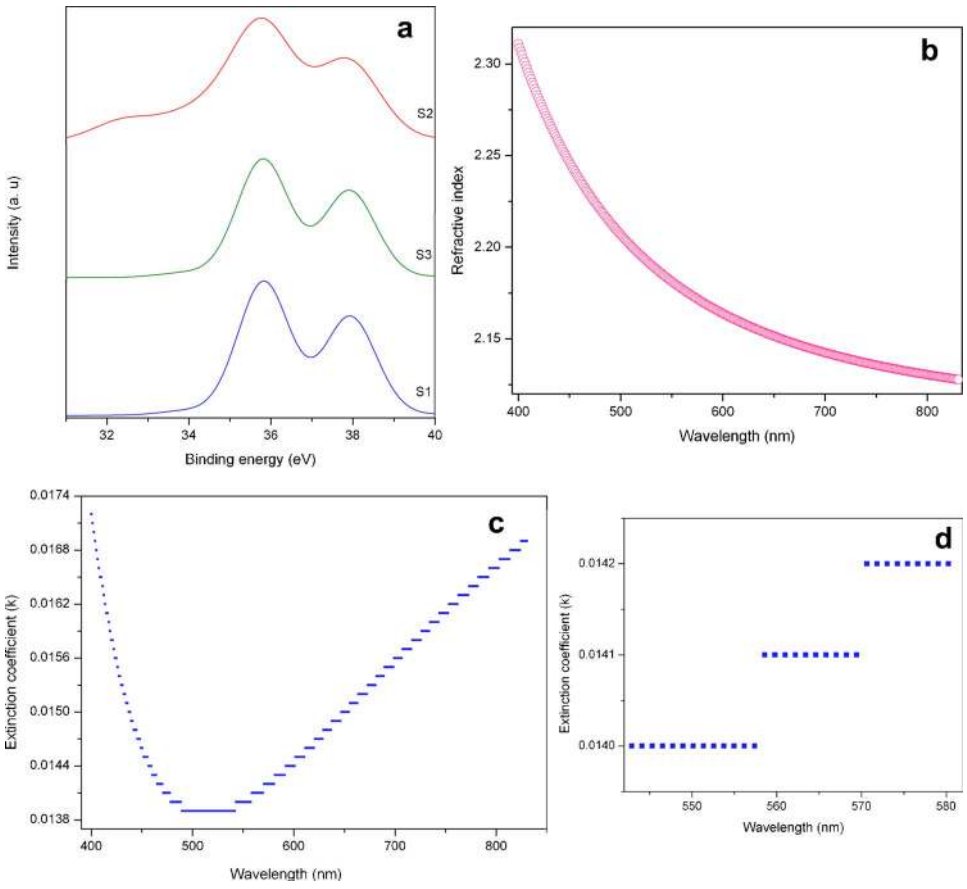

FIG. 3. (Color online) (a) XPS spectrum of the as-deposited (S1) and electron bombarded (S2, S3) WO_3 thin films in the region of W 4*f* levels. (b) Refractive index of sample S1 as a function of wavelength. (c) Spectral dependence of extinction coefficient for the as-deposited tungsten oxide thin films. (d) Extended view of *k* values showing the individual data points in each step.

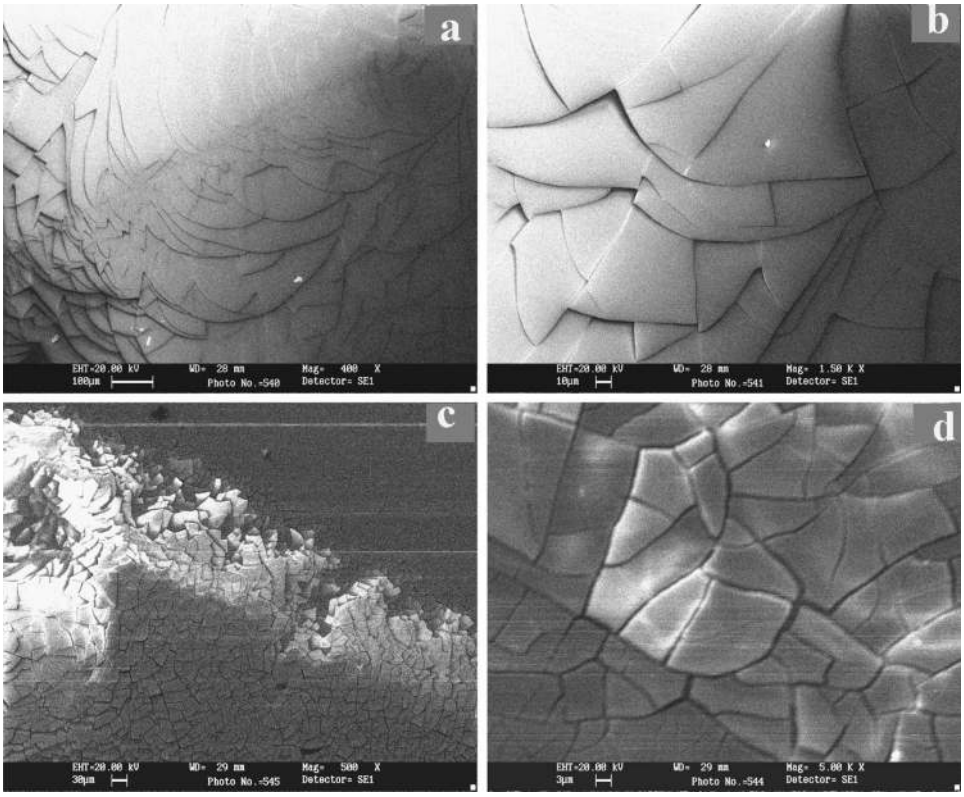

FIG. 4. (a) SEM image of the as-deposited tungsten oxide thin film showing layered structure along the edge of the film. (b) Extended view of the layered structure in S1. (c) The low magnification image of the electron bombarded sample S3. (d) High-magnification SEM image of sample S3 showing cracks at the point of electron impingement.

around the point of impingement turns blue, showing a maximum transmittance of 21% at $\lambda=477$ nm. Interestingly, the band edge of S3 sample is blueshifted by 60 nm. Coloration of the film by electron impingement is attributed to the reduction of WO_3 subsequently leading to the release of oxygen atoms from the sample.[8] Each oxygen vacancy contributes a maximum of two free electrons;[9] hence, the extraction of oxygen atoms by electron bombardment increases the carrier concentration considerably. Thus, the blueshift in S3 sample can be ascribed to the conventional Burstein-Moss effect.[10,11] Similar results have been reported for the WO_3 thin films colored by proton/lithium intercalation.[12] However, understanding of the redshift observed in S2 sample requires more investigation.

In our samples, the release of oxygen atoms by electron bombardment has been confirmed by evaluating the chemical composition of the samples by x-ray photoelectron spectroscopy (XPS) measurements. As shown in Fig. 3(a), the XPS spectrum of the as-deposited sample (S1) shows two peaks with binding energies of 35.8 and 37.9 eV, corresponding to W $4f_{7/2}$ and W $4f_{5/2}$, respectively. They are the valence state peaks of W^{6+} corresponding to the standard spectra of WO_3.[13] But, when the sample is bombarded with electron beam, the spectrum becomes broader showing additional peaks, which create a shoulder at the lower binding energy side. In samples S2 and S3, the shoulder is found approximately at 32.3 and 33.4 eV, respectively. In addition, the valley of the original doublet is also diminished considerably. These changes in the spectra are interpreted in earlier reports as a consequence of nonstoichiometric conditions on the film surface, which may be due to the formation of surface oxygen vacancies.[14] All these results suggest the occurrence of compounds with less oxygen-to-tungsten ratio by electron bombardment.

Figure 3(b) shows the refractive index of as-deposited WO_3 thin film as a function of wavelength [400–850 nm]. The experimental values of n are in fair agreement with the reported values[5] for WO_3 thin films. But, interestingly, the wavelength dependence of extinction coefficient k shows steplike features as shown in Figs. 3(c) and 3(d). The reason for such a behavior is not clear yet; but it is presumed to be associated with the layered structure. A detailed investigation is in progress.

The surface morphology of WO_3 thin films has been studied by scanning electron microscope (SEM) and atomic force microscope (AFM) measurements. The surface of the as-deposited sample S1 is found to be smooth at the center but, along the edges, it shows a layered structure [Fig. 4(a)]. Several platelets are found to be stacked uniformly one over the other. The platelets are found to have different sizes and shapes, but interestingly, all the platelets have nearly same thickness as shown in Fig. 4(b) The possible mechanism of layered growth may be understood from the active arc suppression mechanism of the pulsing unit: Sparc-LE 20. When charges build on the target due to surface oxidation, the pulsing unit reverses the target voltage for $\sim 10\ \mu$s. However, reversal of the target voltage attracts more electrons, subsequently leading to the discharge of positively charged insulative layer. This action lowers the surface potential of the insulative layer and thus prevents the breakdown of an arc. Once the arc is suppressed, the Sparc-LE unit reverses the target voltage back to negative potential and normal sputtering is resumed. Thus, the reduction of sputtering rate by

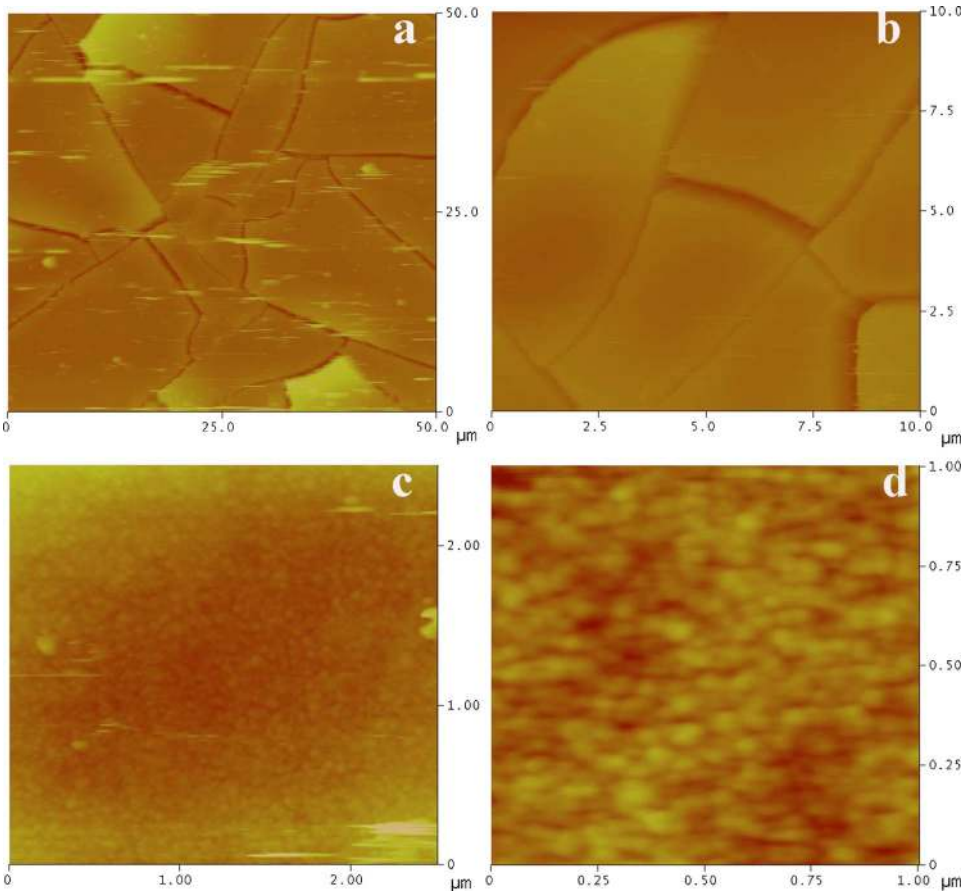

FIG. 5. (Color online) (a)–(d) The AFM images of electron bombarded sample S3 taken at different magnifications.

target poisoning along with the reversal of target voltage for a few microseconds is thought to initiate layer growth in the present investigation. The uniform thickness of the platelets indicates that the target is charged up at regular intervals. The surface morphology of electron bombarded samples S2 and S3 is alike, so a detailed analysis of S3 alone is presented here. When electron beam is irradiated on the film, cracks start developing at the point of impingement and

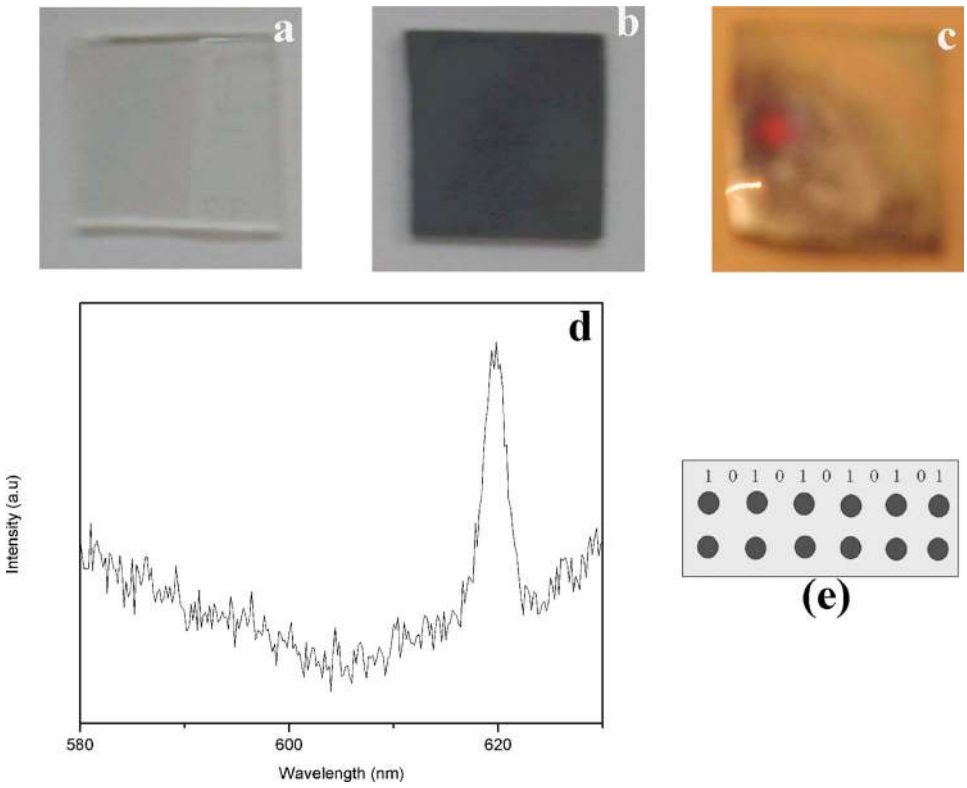

FIG. 6. (Color online) The photographs of the (a) as-deposited sample S1; (b) colored sample S2; and (c) light-emitting sample S3. (d) The PL spectrum of sample S3 excited at $\lambda = 325$ nm. (e) Outline for data storage application based on the coloration/luminescence of WO_3 thin films by electron bombardment.

spread all along the film as shown in Fig. 4(c). The high-magnification SEM image taken at the center of the film shows flakes of different dimensions [Fig. 4(d)]. The cracks probably originate from the strain induced by the difference in thermal expansion between the substrate and the film. A detailed investigation on the crack surface of S3 was done by AFM. At the point of impingement, the surface is found to be smooth with large flakes separated by fine cracks [Fig. 5(a)]. However, the AFM image of a single flake shows a dip at the center with slight elevation along the edges [Fig. 5(b)]. In addition, high-magnification AFM image of individual flakes shows randomly dispersed nanoparticles within the flake [Fig. 5(c)]. The surface crystallite size of the nanoparticles determined from the height image was found to be ~25 nm [Fig. 5(d)].

Apart from the changes in the physical properties, the electron bombardment also gives rise to luminescence. The electron bombarded sample S3 shows intense red emission at $\lambda = 619$ nm. The photographs of the as-deposited (S1), colored (S2), and light-emitting (S3) samples are shown in Figs. 6(a)–6(c). Interestingly, the light emission could not be ascertained to the conventional cathodoluminescence expected from electron bombardment. Rather, the emission is found to be photoluminescence (PL) from the structural modifications (tungsten oxide nanoparticles) and defect sites induced by electron bombardment. Figure 6(d) shows the PL spectrum of S3 sample excited at 325 nm. The band-to-band emission was observed at 357 nm; for the sake of clarity, the spectrum showing red emission alone is presented here. The intense red emission is attributed to the transitions due to localized sites induced by the presence of oxygen vacancies and defects in WO_3 film.[15] All the above results clearly indicate that the electron bombardment of WO_3 thin films leads to significant changes in the structural, optical, and morphological properties. With the optimization of nanostructured electron emitters (nanorods, nanowires, and nanotubes), the coloration and luminescence induced by electron bombardment can be used for data storage. The concept for data storage using electron bombardment is shown in Fig. 6(e). The colored/luminescent portion of the film can be treated as binary "1" and the as-deposited portion as "0," or vice versa. As the electrons can be focused to a fine beam (approximately a few tens of nanometers), it is possible to achieve ultrahigh-density data storage using this method, if optimized.

CONCLUSION

To summarize, tungsten oxide thin films have been deposited by pulsed dc magnetron sputtering in active arc suppression mode. The as-deposited films are found to be amorphous and highly transparent. Along the edges, the film shows a layered structure, which is thought to be the reason for steplike behavior in k values. The structural, optical, and morphological properties of the WO_3 film have been changed by electron beam irradiation. The deep coloration and intense red emission induced by electron bombardment has been proposed for high-density data storage applications.

[1] C. G. Granqvist, A. Azens, P. Heszler, L. B. Kish and L. Österlund, Sol. Energy Mater. Sol. Cells **91**, 355 (2007).
[2] H. Qiu, Y. F. Lu, and Z. H. Mai, J. Appl. Phys. **91**, 440 (2002).
[3] T. Aoki, T. Matsushita, A. Suzuki, K. Tanabe, and M. Okuda, Thin Solid Films **509**, 107 (2006).
[4] T. T. Lin and D. Lichtman, J. Appl. Phys. **50**, 1298 (1979).
[5] E. O. Zayim and N. D. Baydogan, Sol. Energy Mater. Sol. Cells **90**, 402 (2006).
[6] Y. Zhao, Z. C. Feng, Y. Liang, and H. W. Sheng, Appl. Phys. Lett. **71**, 2227 (1997).
[7] A. Karuppasamy and A. Subrahmanyam, Mater. Lett. **61**, 1256 (2007).
[8] H. Morita, T. Miura, and H. Washida, Jpn. J. Appl. Phys. **20**, L323 (1981).
[9] G. A. Niklasson, L. Berggren, and A-L. Larsson, Sol. Energy Mater. Sol. Cells **84**, 315 (2004).
[10] E. Burstein, Phys. Rev. **93**, 632 (1954).
[11] T. S. Moss, Proc. Phys. Soc. London, Sect. B **67**, 775 (1954).
[12] M. Deepa, P. Singh, S. N. Sharma, and S. A. Agnihotry, Sol. Energy Mater. Sol. Cells **90**, 2665 (2006).
[13] J. Scarminio, M. A. B. Moraes, R. C. E. Dias, F. P. Rouxinol, and S. F. Durrant, Electrochem. Solid-State Lett. **6**, H9 (2003).
[14] S. Santucci, L. Lozzi, M. Passacantando, S. D. Nardo, A. R. Phani, C. Cantalini, and M. Pelino, J. Vac. Sci. Technol. A **17**, 644 (1999).
[15] M. Feng, A. L. Pan, H. R. Zhang, Z. A. Li, F. Liu, H. W. Liu, D. X. Shi, B. S. Zou, and H. J. Gao, Appl. Phys. Lett. **86**, 141901 (2005).